Unblocking the effect of crystallinity on rapid sodium storage of digallium trisulfide/carbon nanowires

Danni Du[a1], Xiaoyu Zhang[a1], Minghao Hua[b1], Yuzhuo Chen[a], Yafei Li[a], Chengxiang Wang[a], Xiaohang Lin[a]*, Yuanchang Shi[a]*, Yuanwei Sun[c]*, Jinfeng Sun[d]*, Lidong Yang [e], Longwei Yin[a], Rutao Wang[a]*

[a] Shandong Provincial Key Laboratory of Electrochemical Catalysis and Conversion, State Key Laboratory of Coatings for Advanced Equipment, School of Materials Science and Engineering, Shandong University, Jinan 250100, China

[b] School of Traffic Management Engineering, Shandong Police College, Jinan, 250014, China

[c] Medical Science and Technology Innovation Center & Electron Microscopy Center, Shandong First Medical University & Shandong Academy of Medical Sciences, Jinan, Shandong，250117, China

[d] School of Material Science & Engineering, University of Jinan, Jinan 250024, China

[e] Department of Industrial and Systems Engineering, The Hong Kong Polytechnic University, Hong Kong, China

*Email: rtwang@sdu.edu.cn (R. W.); lxh12345@sdu.edu.cn (X. L.); yuanchangshi@sdu.edu.cn (Y. S.); mse_sunjf@ujn.edu.cn (J. S.); ywsun@sdfmu.edu.cn (Y. S.).

Experimental Section

Synthesis of gallium metal organic framework nanowires (Ga-MOF)

Ga-MOF was synthesized via a simple solvothermal method. First, $Ga(NO_3)_3 \cdot xH_2O$ (1 g) was dissolved into DMF solution under vigorous stirring at ambient temperature. After that, 1,4-benzenedicarboxylic acid (2g) and 1,2-benzisothiazolin-3-one (2 g) were then dissolved into the above solution. Then, the solution was put into hydrothermal reactor which was heated in an oven about 10 h at 120 °C. After the cooling, the achieved white powder was then rinsed with DMF and deionized water and dried in a freezing drying for 48 h to acquire Ga-MOF. The above chemicals were achieved from Shanghai Aladdin Biochemical Technology Co., Ltd..

Synthesis of LC-Ga_2S_3 and HC-Ga_2S_3

The Ga-MOF (0.2 g) and S (1g) was placed on both sides of the crucible and then heated in a tube furnace in Ar atmosphere. The heating rate is controlled at 5 ºC min^{-1}. The sample keeps heating at 800 ºC for 1 hour. After cooling down, the collection of black products is the low crystallinity Ga_2S_3 (named LC-Ga_2S_3). Similarity, the high crystallinity Ga_2S_3 was synthesized at 900 °C for 1 h (named HC-Ga_2S_3).

Characterization

Morphological analysis was carried using a FESEM (JSM-7800F, JEOL, Japan). The structure of Ga_2S_3 with different degrees of crystallinity and the element mappings were investigated by means of TEM (JEM-F200, JEOL, Japan). In situ transmission electron microscopy (TEM, Talos F200i, FEI, USA) was analyzed to quantify the volume changes and transport velocities during the embedding of sodium in the material. The crystal structure and phase composition of the as-synthesized Ga-MOF precursor and Ga_2S_3 samples were characterized by XRD using a DMAX-2500PC diffractometer with Cu-Kα radiation (λ = 1.5405 Å) at a scanning rate of 10° min^{-1}. For the electrochemical analysis, in situ XRD patterns of the LC-Ga_2S_3 and HC-Ga_2S_3 electrodes were collected during the first cycle over a 2θ range of 5° to 60° at a scan speed of 5° min^{-1}, using a Be foil as the current collector. The charge/discharge processes were conducted at 0.1 A g^{-1}. Raman spectra were recorded on a JY-HR800 spectrometer (France) with an excitation wavelength of 532 nm. The surface chemical composition of the Ga_2S_3 samples was examined by XPS on an AXIS Supra instrument (UK). Nitrogen adsorption-

desorption isotherms were measured to determine the SSA and PSD of the Ga_2S_3 samples using the BET method. TGA was performed on a DSC8000 (Perkin Elmer) instrument at a heating rate of 10 °C min^{-1} in air to evaluate the thermal stability and carbon content of the materials. The defect status of the samples at room temperature was performed by EPR spectrometer (EPR, Bruker-E500, German).

Electrochemical measurements

CR2032 cells assembled in an argon-filled glove box (< 0.01 ppm of moisture and oxygen contents) were used to test the electrochemical performance. For all cells, glass-fiber membrane (Whatman GF/D) was employed as the separator. The electrolyte is 1 M $NaPF_6$ in DME. Active materials (e.g., LC-Ga_2S_3/C), carbon black, and carboxymethylcellulose (CMC) were blended in a weight ratio of 8:1:1 with a bit water. Then mixture was bladed on a Cu foil and dried in a vacuum at 80℃. The active mass loading on Cu foil is ~0.7-1.0 mg cm^{-2}. Homemade porous carbon (PC), super P, and PVDF were blended in a weight ratio of 8:1:1 and then rolled into thin sheets, followed by drying in a vacuum at 120℃. For half cells, a Na foil was utilized as counter electrode and the prepared active materials served as the cathode. For assembling SICs, the as-prepared active materials, and PC, were used as negative and positive electrodes, respectively. The active mass loading ratio was approximatively 1:1 of the anode and PC. Before the assembly of SICs, the anode was conducted by several discharged-charged cycles at 0.1 A g^{-1} in the half cell then achieved by detached in the glove box. The charge/discharge testes were measured by a battery test system (LAND) at RT. CV curves were performed on a CHI760E electrochemical workstation. EIS measurements spanned 10^{-2} Hz to 10^5 Hz. GITT tests were conducted by the operating cells at 0.1 A g^{-1} for 5 min and rest intervals for 25 min in the range of 0.01 to 3.0 V.

Calculation of the specific energy and power

The energy and power densities (E, P) of the SIHC full cells were calculated using the following equations:

$$E = \int_{t1}^{t2} VIdt = \frac{V_{max} + V_{min}}{2} \times It \times \frac{1}{3600} \quad (1)$$

$$P = \frac{3600E}{t} \quad (2)$$

where t represents the discharged time, i is the current density, V_{max} is the beginning potential with considering the current resistance (IR) drop, and V_{min} is the end potential of discharge.

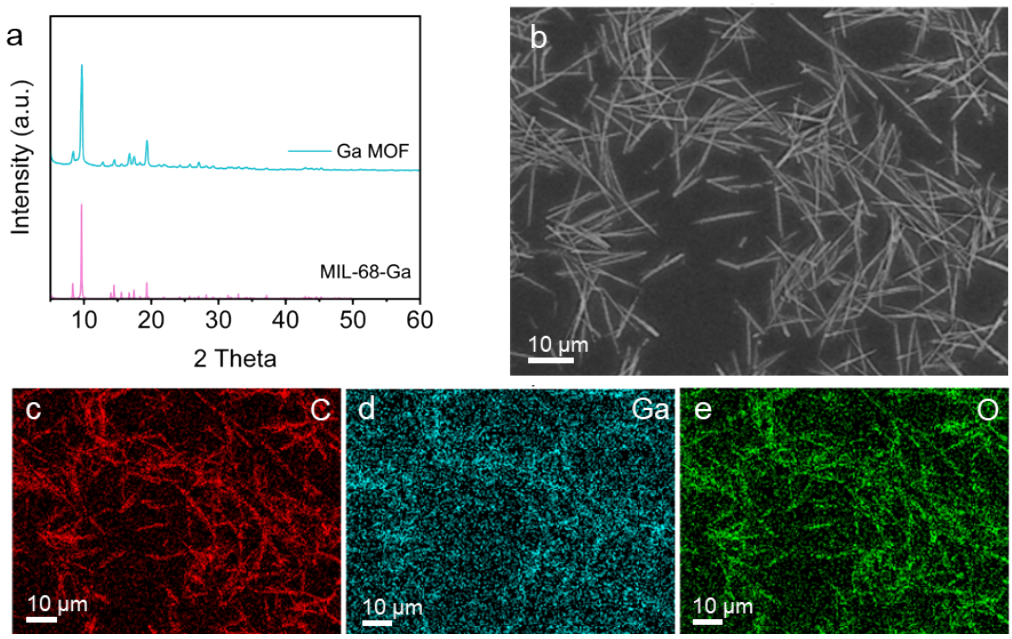

Fig. S1 (a) XRD pattern of MIL-68-Ga MOF. **(b)** SEM image of MIL-68-Ga MOF and the corresponding EDS mapping: **(c)** C, **(d)** Ga, and **(e)** O.

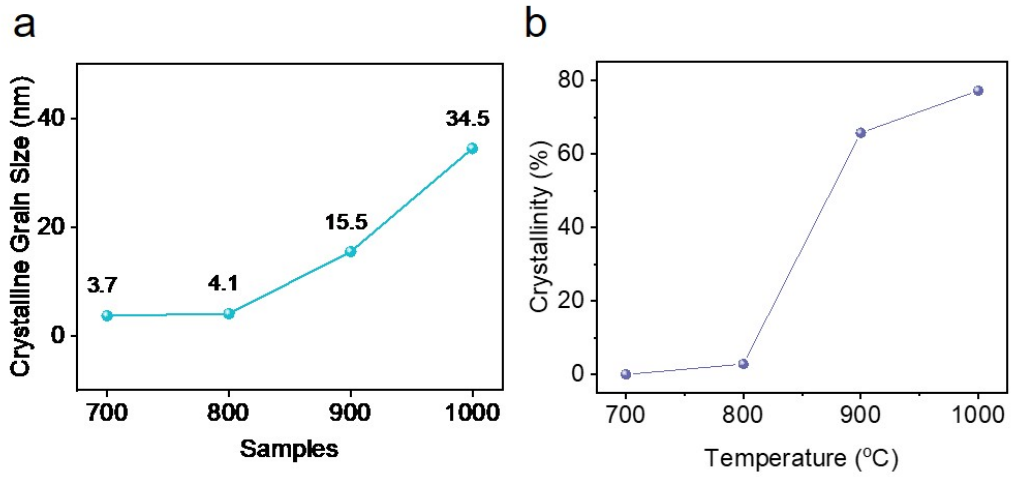

Fig. S2 (a) The evaluated average crystalline grain sizes for Ga_2S_3/C samples from XRD spectrum. **(b)** The calculated degrees of crystallinity from JADE for these Ga_2S_3/C samples achieved at the different temperatures.

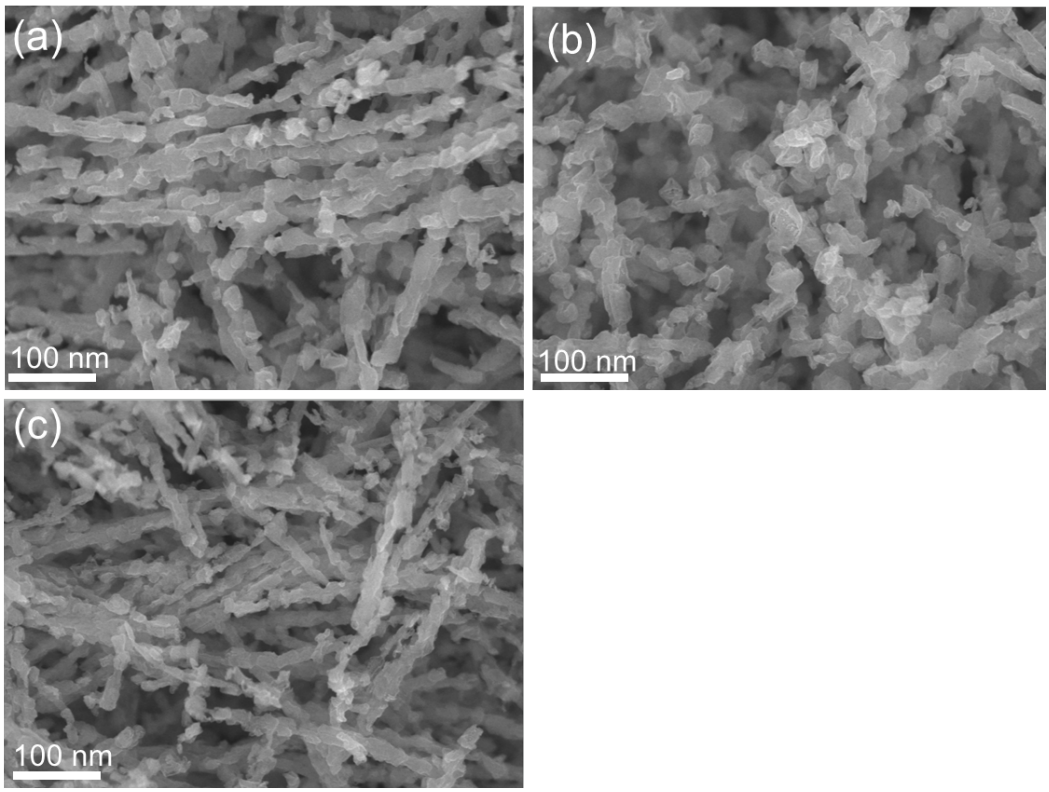

Fig. S3 SEM images of Ga_2S_3/C samples under the different heating temperatures: (a) 800 ℃, **(b)** 900 ℃, **(c)** 1000 ℃.

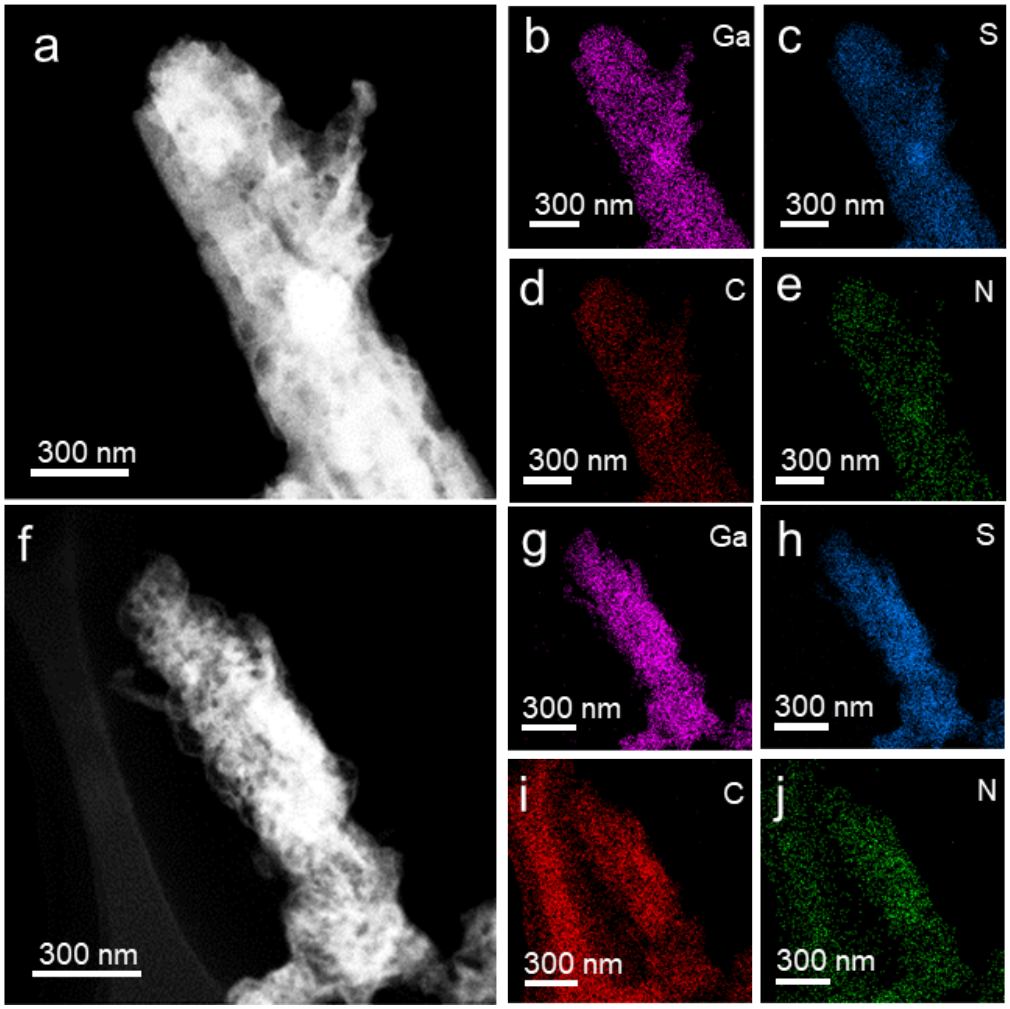

Fig. S4 (a) ADF-STEM image of LC-Ga_2S_3/C and the corresponding EDS mapping image: **(b)** Ga, **(c)** S, **(d)** C and **(e)** N. **(f)** ADF-STEM image of HC-Ga_2S_3/C and the corresponding EDS mapping image: **(g)** Ga, **(h)** S, **(i)** C and **(j)** N.

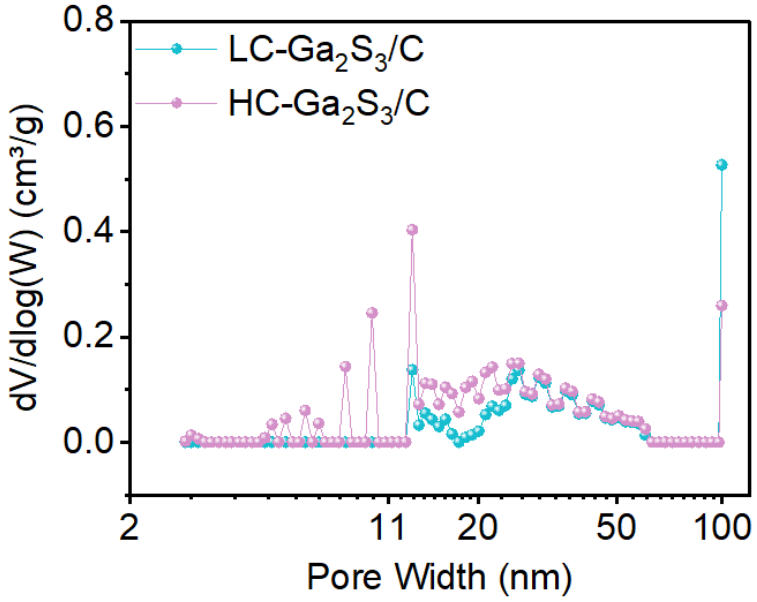

Fig. S5 PSD curves of LC-Ga_2S_3/C and HC-Ga_2S_3/C.

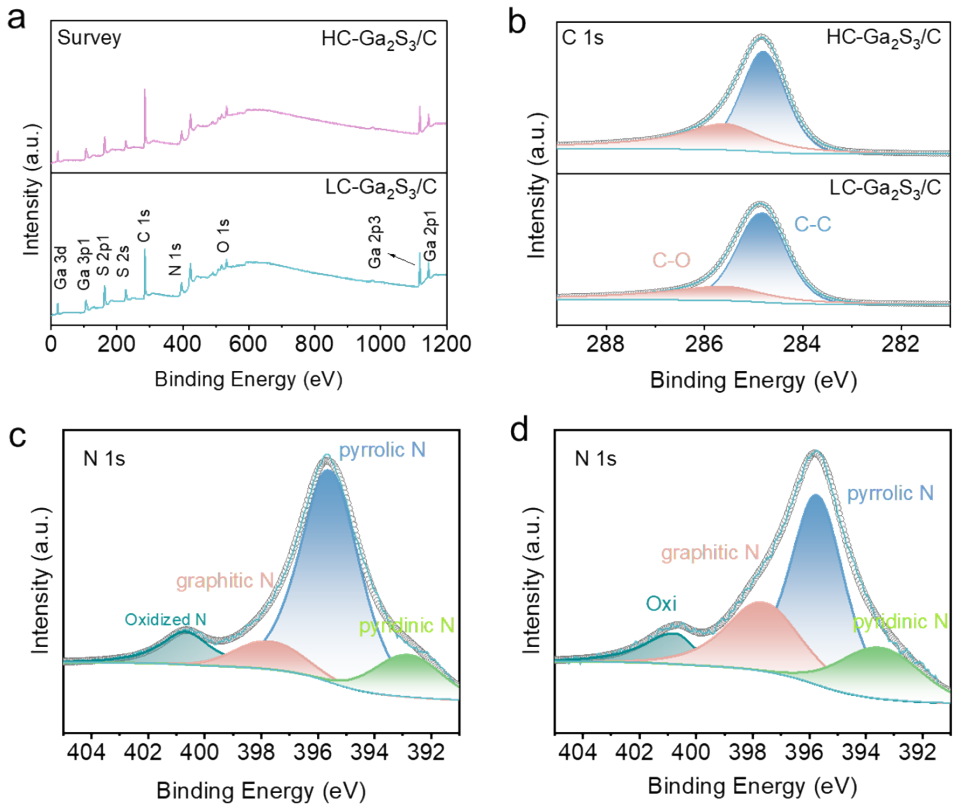

Fig. S6. **XPS spectrum of LC-Ga_2S_3/C and HC-Ga_2S_3/C: (a)** Full-scale XPS spectrum. **(b)** High-resolution C1s spectrum, **(c)** High-resolution N1s spectrum for LC-Ga_2S_3/C, **(d)** High-resolution N1s spectrum for HC-Ga_2S_3/C.

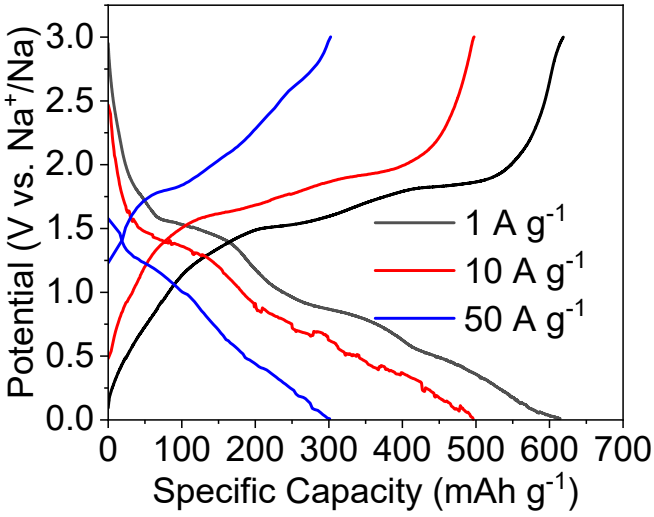

Fig. S7 Typical GCD curves of LC-Ga_2S_3/C electrode at high current densities.

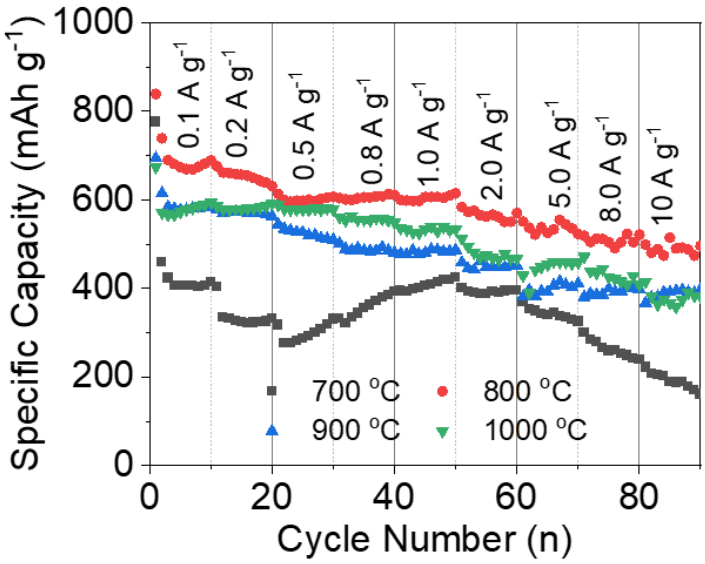

Fig. S8 The rate performances of Ga_2S_3/C samples prepared at different heating temperatures.

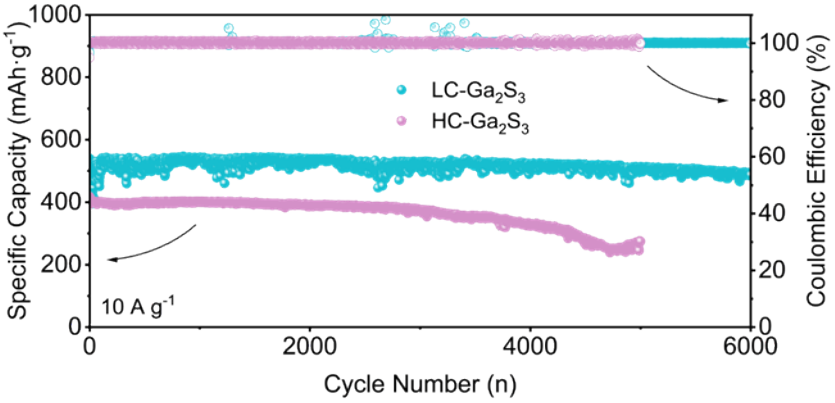

Fig. S9 The rate performances of Ga_2S_3/C samples prepared at different heating temperatures.

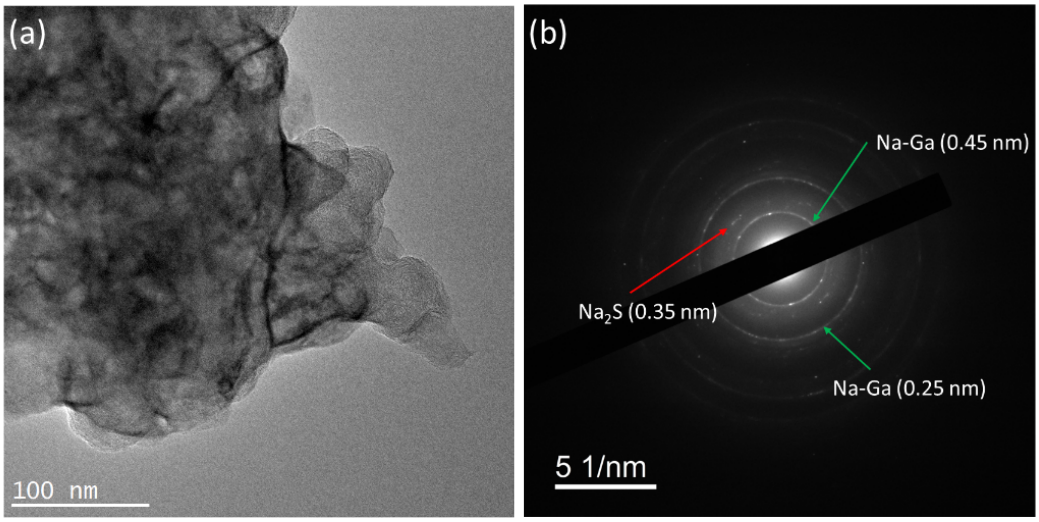

Fig. S10 (a) TEM image of LC-Ga_2S_3/C achieved at 0.01 V and **(b)** the corresponding SAED pattern.

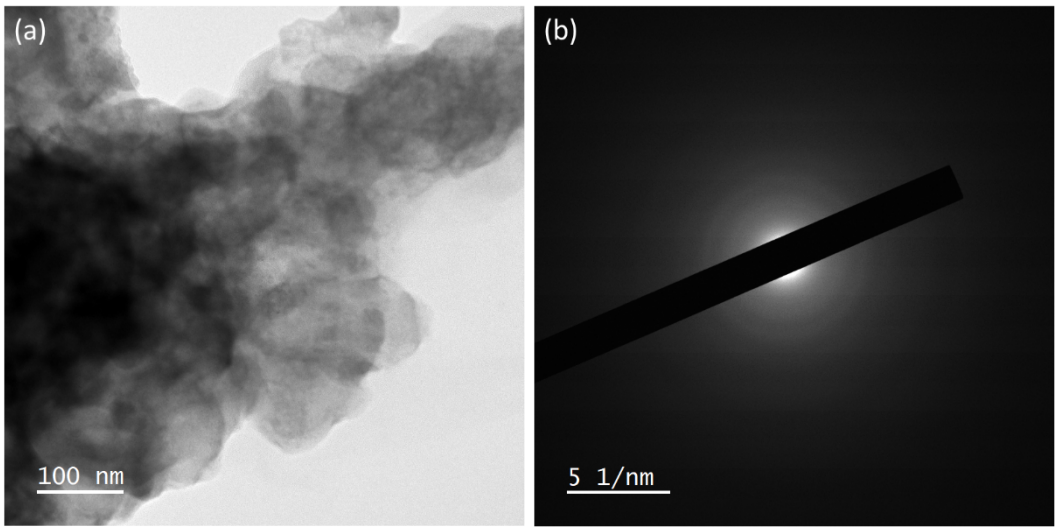

Fig. S11 (a) TEM image of LC-Ga_2S_3/C achieved at 3.00 V and **(b)** the corresponding SAED pattern.

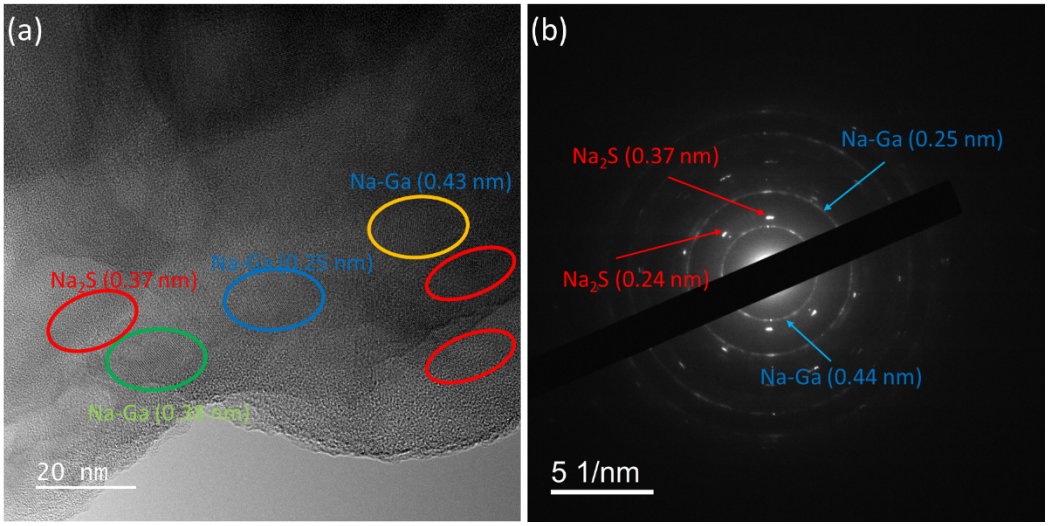

Fig. S12 (a) TEM image of HC-Ga_2S_3/C achieved at 0.01 V and **(b)** the corresponding SAED pattern.

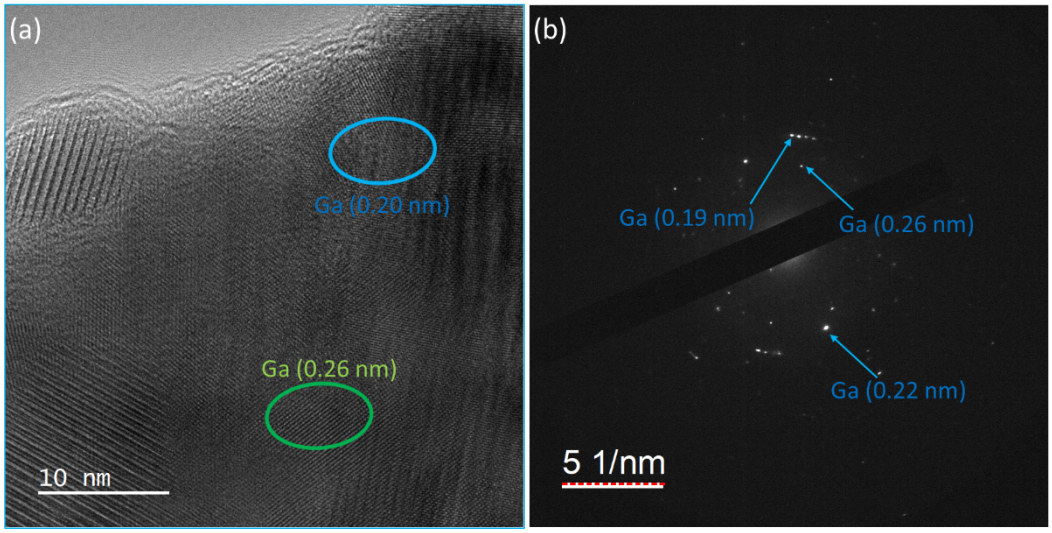

Fig. S13 (a) TEM image of HC-Ga_2S_3/C achieved at 3.00 V and **(b)** the corresponding SAED pattern.

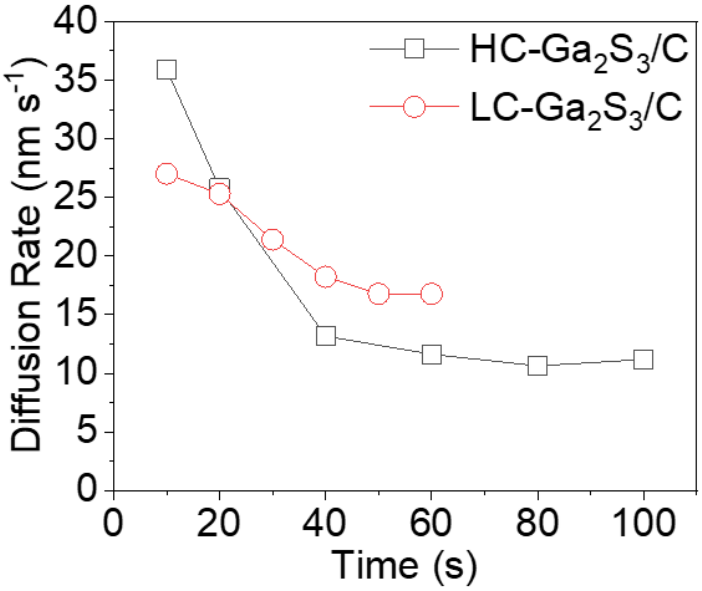

Fig. S14 The Na^+ diffusion rates for LC-Ga_2S_3/C and HC-Ga_2S_3/C along the axial direction. Na^+ moves across LC-Ga_2S_3/C nanowires (Screenshot area) with a time of ~60 s, while Na^+ moves across HC-Ga_2S_3/C nanowires (Screenshot area) with a longer time of ~100 s.

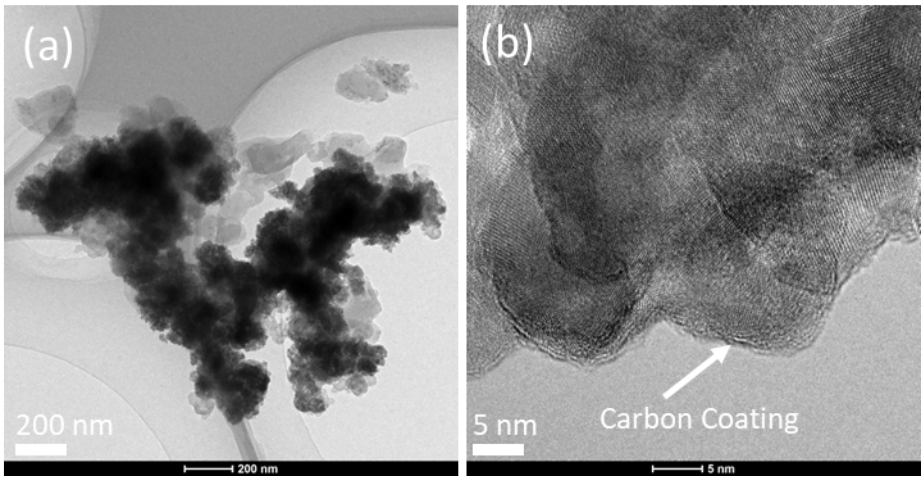

Fig. S15 TEM images of LC-Ga_2S_3/C after 1000 cycles.

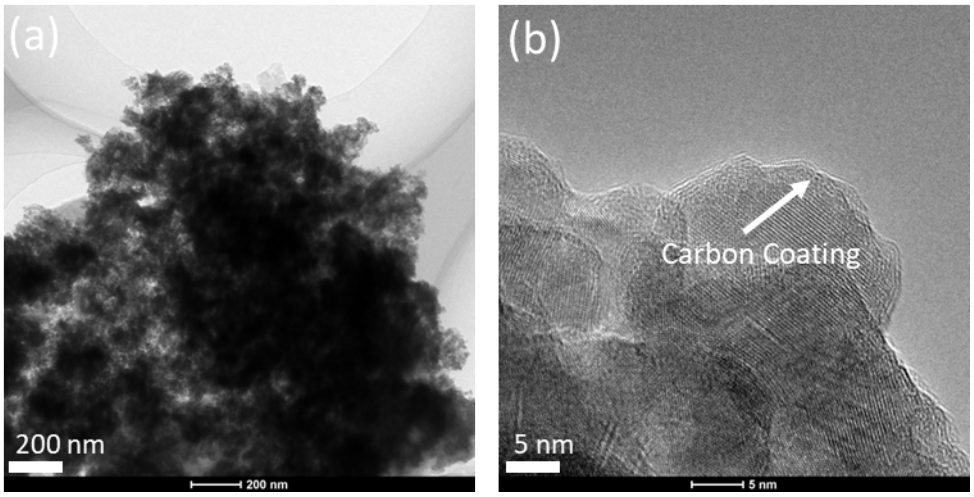

Fig. S16 TEM images of HC-Ga_2S_3/C after 1000 cycles.

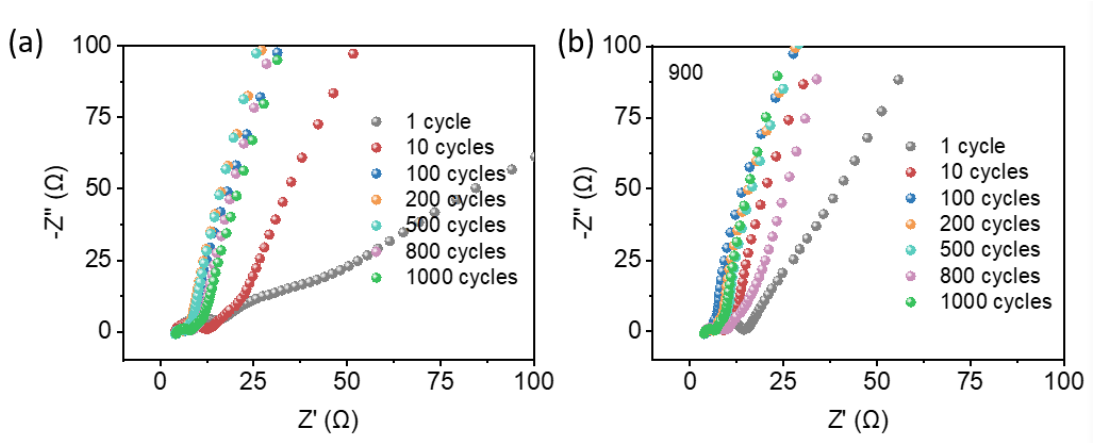

Fig. S17 EIS spectra achieved at different cycling stages: (a) LC-Ga_2S_3/C and **(b)** HC-Ga_2S_3/C.

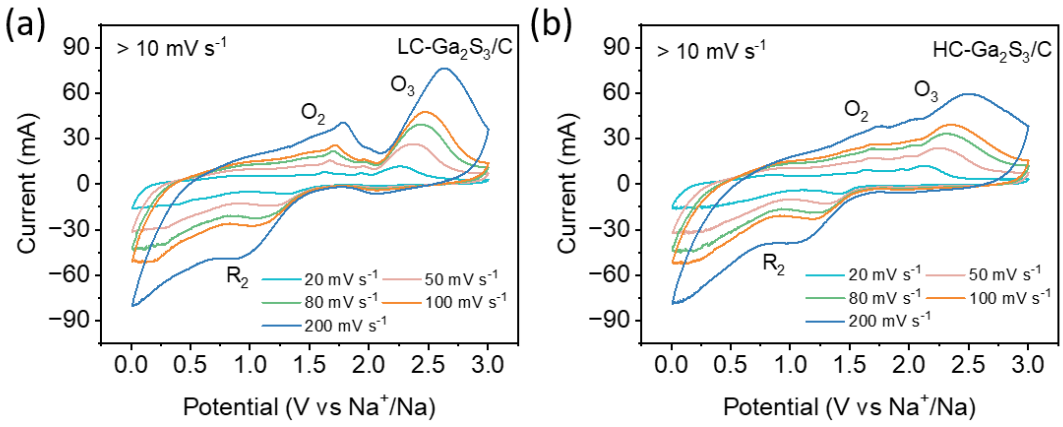

Fig. S18 CV curves at the high sweep rates: (a) LC-Ga_2S_3/C and **(b)** HC-Ga_2S_3/C

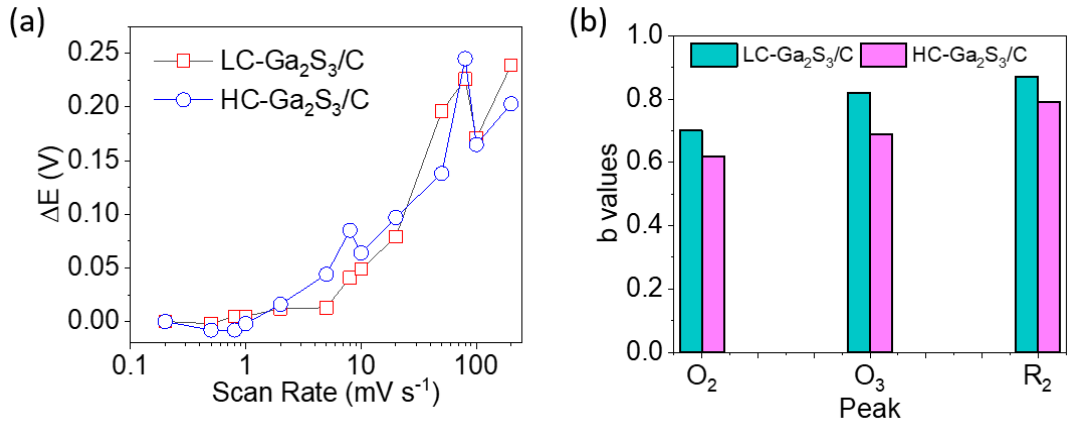

Fig. S19 (a) O_2 peak shift along with increasing scan rate for LC-Ga_2S_3/C and HC-Ga_2S_3/C. **(b)** b values for O_2, O_3, and R_2 peaks at the high scan rate from 20 to 200 mV s^{-1}. Noted that b values are absent due to that O1 and R1 peaks become undistinguishable especially at high rates shown in Fig. S18.

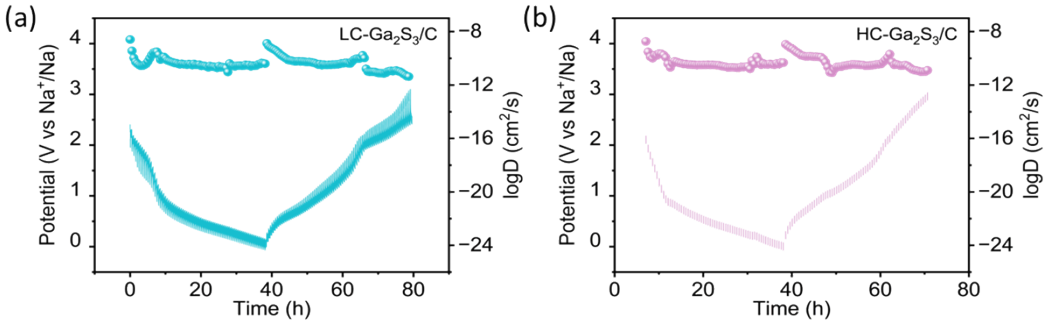

Fig. S20 GITT curves and the corresponding D values for (a) LC-Ga_2S_3/C and **(b)** HC-Ga_2S_3/C.

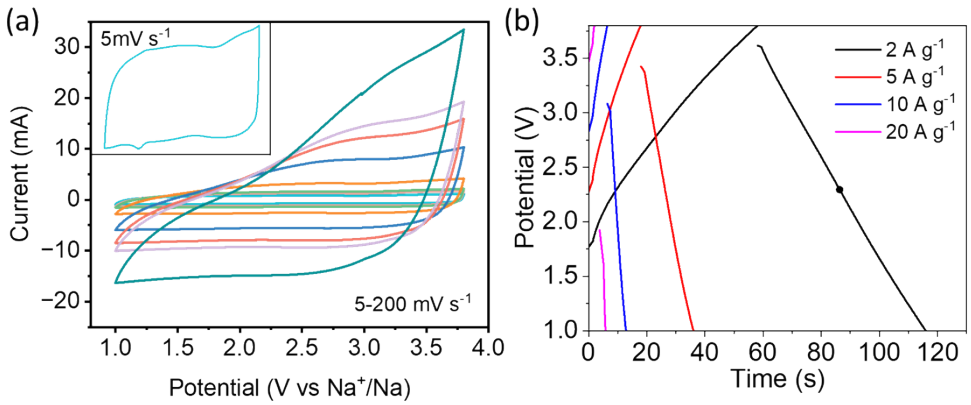

Fig. S21(a) CV curves of LC-Ga_2S_3/C//PC SIC. **(b)** GCD curves of LC-Ga_2S_3/C//PC SIC at high current densities.